

This is a provisional PDF only. Copyedited and fully formatted version will be made available soon.



**ISSN:** 0015-5659

**e-ISSN:** 1644-3284

## **Cardioprotective effect of phytosterol stigmasterol supplementation against doxorubicin-induced cardiotoxicity**

**Author:** Ying Wang

**DOI:** 10.5603/fm.103866

**Article type:** Original article

**Submitted:** 2024-12-02

**Accepted:** 2025-02-18

**Published online:** 2025-03-25

This article has been peer reviewed and published immediately upon acceptance. It is an open access article, which means that it can be downloaded, printed, and distributed freely, provided the work is properly cited. Articles in "Folia Morphologica" are listed in PubMed.



## ORIGINAL ARTICLE

Ying Wang, Cardioprotective effect of stigmasterol

### **Cardioprotective effect of phytosterol stigmasterol supplementation against doxorubicin-induced cardiotoxicity**

Ying Wang

Inner Mongolia Autonomous Region People's Hospital, Department of Hematology, Hohhot, Inner Mongolia, Autonomous Region, China

**Address for correspondence:** Ying Wang, Inner Mongolia Autonomous Region People's Hospital, Department of Hematology, No. 20 Zhaowuda Road, Hohhot 010020, Inner Mongolia Autonomous Region, China; e-mail: cfwy1980@outlook.com

#### **ABSTRACT**

**Background and objectives:** Stigmasterol, a phytosterol abundantly found in various plant sources, including soybeans and other legumes, plays a significant pharmaceutical role due to its pharmacological properties. Research suggests that stigmasterol exhibits anti-inflammatory, antioxidant, and cholesterol-lowering effects, making it a promising candidate for managing cardiovascular disorders. In this work, we elucidated the cardioprotective potency of stigmasterol against doxorubicin-induced cardiotoxicity in rats.

**Materials and methods:** Hence we have evaluated the potency of stigmasterol supplementation in preventing doxorubicin-induced cardiotoxicity. Male Wistar rats were treated with doxorubicin (2.5 mg/kg) and supplemented with 25 and 50 mg/kg doses of stigmasterol for 14 days. On 14<sup>th</sup> day of treatment tail-cuff plethysmography was conducted to assess the hemodynamic parameters. The concentrations of oxidative stress markers, cardiac function markers, myocardial damage markers, and inflammatory biomarkers were assessed in the experimental rats using the commercial kits. The heart tissues were subjected to the histopathological analysis. Docking study was also conducted with NF- $\kappa$ B.

**Results:** The stigmasterol treatment effectively increased the body weight and heart weight and elevated the hemodynamic parameters in doxorubicin-induced rats. The stigmasterol treatment also decreased the oxidative stress via increasing antioxidants, reduced the cardiac function markers, and decreased the myocardial damage markers in the doxorubicin-induced rats. Furthermore, the stigmasterol treatment also reduced the inflammatory markers in the doxorubicin-induced rats. The cardioprotective properties of the stigmasterol was further supported by the results of histopathological analysis and docking analysis where it showed excellent binding affinity for NF- $\kappa$ B.

**Conclusions:** The results of tail-cuff plethysmography and cardiac tissue histopathological analysis authentically proved the inhibitory effect of stigmasterol against doxorubicin induced cardiotoxicity. To conclude supplementation with phytochemical stigmasterol persuasively ameliorated doxorubicin induced cardiotoxicity.

**Keywords:** anticancer drug, doxorubicin, cardiotoxicity, phytosterol, stigmasterol, supplementary drug

## INTRODUCTION

Cancer remains one of the most lethal diseases, claiming numerous lives annually worldwide. Effective management of this illness is influenced by its diverse manifestations globally, the accessibility of medical resources, and various socioeconomic factors [12]. Projections based on global cancer statistics suggest a staggering rise in cases, with an estimated 20 million additional diagnoses and 10 million deaths attributed to cancer [32]. Such predictions indicate a looming 60% surge in the burden of cancer over the next two decades, posing significant challenges to communities, individuals, and healthcare systems alike. Currently available anticancer drugs encompass a diverse array of pharmaceutical agents designed to target various aspects of cancer biology and progression. These drugs include traditional cytotoxic chemotherapy drugs, such as anthracyclines and taxanes, targeted therapies, immunotherapy drugs and hormonal therapies [7, 38]. However, challenges remain, including drug resistance and toxicity, highlighting the ongoing need for continued research and development of novel therapeutic strategies.

Doxorubicin (DOX) has exhibited notable therapeutic efficacy and is acknowledged as a highly effective chemotherapy agent from 1974 which was accepted by the Food and Drug

Administration (FDA) for combating a range of tumors [15]. Its indications include breast cancer, carcinomas, sarcomas, and hematological malignancies, underscoring its versatility in cancer treatment. Despite the widespread use of anthracyclines, their adverse effects on vital organs like brain, liver, kidney and it is manifold with cardiotoxicity being the most prominent and extensively researched [20, 40].

Doxorubicin induced toxicity occurs through various mechanism including oxidative stress caused by reactive oxygen species (ROS), inhibition of topoisomerase II, and the induction of DNA double-strand breaks, resulting in altered gene transcription and apoptosis as well as dysregulation of intracellular calcium levels [15]. In heart oxidative stress stands out as the primary contributor to doxorubicin-induced cardiotoxicity because of its relatively low amounts of antioxidant enzymes, a high density/volume of mitochondria, and an elevated rate of oxygen consumption [30]. Doxorubicin-induced cardiotoxicity can present as arrhythmias, ischemia, systolic dysfunction, and heart failure, primarily stemming from cardiac cell death and necrosis. Various research had explored the supplementation of natural phytochemicals to counteract toxicity induced during cancer chemotherapy [1].

Stigmasterol, a natural phytosterol found abundantly in various plant sources, has gained considerable attention in pharmacological study due to its diverse biological activities and potential health benefits. Pharmacological investigations have revealed several promising therapeutic properties associated with stigmasterol such as analgesia, anti-inflammatory effects, antioxidant, cholesterol-lowering effects, anticancer, neuroprotective effects, anti-diabetic properties, and immunomodulatory activity [3, 9, 39]. In this work, we elucidated the cardioprotective potency of stigmasterol against doxorubicin-induced cardiotoxicity in rats.

## **MATERIALS AND METHODS**

### **Chemicals**

The drugs Stigmasterol (purity: 95%) and Doxorubicin hydrochloride (purity: 98%) were obtained from Sigma-Chemicals, USA. All the chemicals and reagents utilized in the present investigation are of analytical grade.

### **Experimental animals**

In this work, 8-week-old 24 healthy male Wistar rats were utilized, and their average weight ranged from 140–210 grams. These rats were housed in confines under regulated conditions with a temperature of 25°C and a 12-h light/dark series. They had continuous access to water and standard laboratory meal pellets. A duration of two weeks was given to the rats to acclimatize without any disturbance. The study protocol was verified by the ethical committee. All procedures conducted during the experiment adhered to the regulations for the ethical handling and utilization of laboratory animals.

### **Animal grouping**

The rats were distributed into four groups, each consisting of six individuals. Group 1, serving as the control, administered (i.p.) only normal saline 0.9% for 14 days. In Group II, rats were induced with acute cardiotoxicity by administering doxorubicin intraperitoneally at a dosage of 2.5 mg/kg every other day for two weeks. Groups III and IV received stigmasterol supplementation at 25 and 50 mg/kg concentrations intraperitoneally, respectively, concurrently with doxorubicin treatment. On 14<sup>th</sup> day of treatment tail-cuff plethysmography was conducted to assess cardiovascular function. Twenty-four hours after the final injection, the rats were anesthetized with 50 mg/kg of ketamine and 5 mg/kg of xylazine (i.p.). Blood samples were obtained via the retroorbital plexus and allowed to clot for 15 minutes before centrifugation at 1500×g and 4°C for 10 min to obtain serum. Following decapitation, the cardiac tissues were removed and then preserved at –80°C for subsequent biochemical and histological analyses.

### **Assessment of total body and organ weight gain**

Twenty-four hours after the final injection, the rats were weighed in the digital weighing machine to assess the total weight gain by the control and treated rats. The meticulously excised hearts from the experimental animals were rinsed with ice-cooled saline, gently dried with filter paper and weighed with digital weighing machine.

### **Analysis of hemodynamic parameters**

The hemodynamic parameters, including heart rate (HR), systolic arterial pressure (SAP), diastolic arterial pressure (DAP), and mean arterial pressure (MAP) were analysed through non-invasive tail-cuff plethysmography with a pressure meter. The animals were gently restrained

with a holder without creating any stress. The tail cuff was carefully placed around the base of the tail without restricting the blood flow. The changes in the tail artery pressure was measured by inflating the cuff and slowly deflating process. The results were interpreted with software provided along with tail-cuff plethysmography.

### **Evaluation of cardiac redox status**

Cardiac tissue homogenate was prepared with ice-cold PBS (pH 7.4) in ratio of 1:10. The suspension was centrifuged  $2000\times g$  for 15min and the supernatant was utilized for the assessment of lipid peroxidation and antioxidant levels in the experimental rats. Lipid peroxidation was quantified with TBARS level and both enzymatic and non-enzymatic antioxidants were quantified in the sample. SOD and CAT were estimated with colorimetric assay kit obtained from Sigma Aldrich. Colorimetric assay kits procured from Cayman Chemicals were used for the estimation of TBARS (#10009055), GST (#703302), GR (#703202), GPx (#703102), and GSH (#703002).

### **Estimation of cardiac markers**

Cardiac markers aspartate aminotransferase activity (#MAK055), lactate dehydrogenase activity (#MAK066), and creatinine kinase activity (#MAK116) were estimated using colorimetric assay kits procured from Sigma Aldrich (St. Louis, MO, USA). The conversion of aspartate to  $\alpha$ -ketoglutarate with the transfer of an amino group generates glutamate, leading to the formation of a colorimetric product was detected at 450 nm, which is directly relative to the enzymatic activity of AST. LDH catalyzes the reduction of NAD to NADH, which was detected by colorimetric estimation at 450 nm. Creatine kinase (CK) activity was assessed through a linked enzyme reaction, leading to the generation of NADPH, whose concentration was measured at 340 nm, indicating the level of CK activity in the sample.

### **Assessment of myocardial damage**

The myocardial damage in the doxorubicin treated rats were assessed with biochemical cardiac damage marker proteins creatine kinase MB enzyme (CK-MB), glycogen phosphorylase isoenzyme BB (GP-BB) and heart-type fatty acid-binding protein (H-FABP) in the serum of experimental animals. The levels were studied commercially available ELISA kits. Creatine

kinase MB enzyme was quantified using the Rat Creatine Kinase MB ELISA Kit (#ab285275) procured from Abcam. Glycogen phosphorylase isoenzyme BB and heart-type fatty acid-binding protein were quantified using Novus Biologicals™ Rat Glycogen Phosphorylase BB/GPBB ELISA Kit (#NBP2-82493) and Biomatik Corporation Rat heart fatty acid binding protein (h-FABP) ELISA Kit (#50-149-8889) respectively procured from fisher scientific. The test were performed in triplicates as per the manual instruction.

### **Estimation of INF- $\gamma$ and MCP-1**

Persistent stimulation of INF- $\gamma$  has been linked to the development of autoimmune myocarditis and inflammatory cardiac ailments. Additionally, heightened MCP-1 levels are correlated with a range of cardiovascular disorders, encompassing atherosclerosis and myocardial infarction. Rat INF- $\gamma$  Kit (#CSB-E04579r) and Rat MCP-1/monocyte chemotactic and activating factor, MCP-1/MCAF ELISA kit (#CSB-E07429r) obtained from CUSABIO was used for the estimation INF- $\gamma$  and MCP-1 respectively in the serum. The assay was done according to the instructions outlined in the manual and the final absorbance was taken at 450 nm. The levels were determined with the standard curve plot.

### **Evaluation diagnostic indicators of cardiac damage**

The diagnostic indicators of cardiac damage TGF- $\beta$ , cTroponinI, and BNP levels in the serum were evaluated with the commercially available assay kits. Rat TGF beta 1 ELISA Kit (#MBS824788) from MyBioSource.com, Rat Cardiac Troponin I ELISA Kit (#ab246529) from Abcam and Rat brain natriuretic peptide BNP ELISA Kit (#CSB-E07972r) from CUSABIO were used to detect concentrations of TGF- $\beta$ , cTroponinI, and BNP respectively.

### **Quantification of inflammatory biomarkers**

The concentrations of TNF- $\alpha$  and IL-1 $\beta$  were studied using the Rat TNF- $\alpha$  ELISA Kit (#RAB0479) Rat IL-1  $\beta$  ELISA Kit (#RAB0277) obtained from Sigma Aldrich. NF- $\kappa$ B transcription factor was estimated with NF $\kappa$ B p65 Transcription Factor Assay Kit (#ab133112) from Abcam. HO-1 (#MBS764989) and NQO1 (#MBS7606601) enzymes involved in inflammatory response were quantified with ELISA kits purchased from MyBioSource.com.

### **Histopathological analysis**

The heart tissues were fixed with Bouin solution for 24h before dehydrating with series of alcohol. It is then subjected to vitrification process using dimethylbenzene. The processed tissue were embedded in paraffin, sectioned into 4micron slices with microtome. The tissue sections were mounted on to clean glass slide and stained using eosin and hematoxylin. The stained sections were analyzed with light microscopy.

### **Docking analysis**

The docking of stigmasterol with NF- $\kappa$ B was performed using CB-Dock using the default setting.

### **Statistical analysis**

Result analysis was performed using GraphPad Prism (version 8.1). Results were expressed as mean  $\pm$  SD. Statistical significance was determined using one-way analysis of variance (ANOVA) followed by Tukey's *post hoc* test. A p-value of 0.05 or less was fixed as significant. \*Control vs doxorubicin alone treated group. \*\*Doxorubicin alone treated group vs 25 mg/kg and 50 mg/kg stigmasterol treated rats.

## **RESULTS**

### **Impact of phytosterol stigmasterol on weight gain in cardiotoxicity induced mice**

Doxorubicin treatment significantly ( $p < 0.01$ ) decreased the total body weight to  $152 \pm 4$  g compared to the control rats which weighed about  $210 \pm 7$  g. Stigmasterol treatment increased the total body weight to  $167 \pm 5$  g and  $189 \pm 4$  g in 25 and 50 mg stigmasterol treatment respectively. Cardiac tissue weight was also decreased in the doxorubicin treated rats to  $0.62 \pm 0.0004$  g whereas the control rats shown  $0.79 \pm 0.0009$  g. 25 mg stigmasterol treated rats shown significant ( $p < 0.05$ ) increase in the cardiac tissue weight to  $0.62 \pm 0.0006$  g and the 50 mg stigmasterol treated rats shown  $0.68 \pm 0.0007$  g which is comparatively equal to the cardiac weight exhibited by the control rats (Fig. 1).

### **Effect of phytosterol stigmasterol on cardiac functioning in cardiotoxicity induced mice**

The hemodynamic parameters in the cardiotoxicity induced and stigmasterol treated mice were measured with tail-cuff plethysmography and the results were illustrated in the Figure 2. Systolic arterial pressure and diastolic arterial pressure were maintained at 148 and 106 mmHg in control rats whereas it is decreased in 87 and 62 mmHg in doxorubicin treated rats. Stigmasterol significantly ( $p < 0.05$ ) increased both systolic and diastolic arterial pressure in cardiotoxicity induced rats compared to the untreated rats. 50mg stigmasterol treated rats shown 132 and 89 systolic and diastolic arterial pressure which is comparatively equal to the control rats arterial pressure. The mean arterial pressure and heart rate was also diminished to 61 and 276 mmHg respectively ( $p < 0.05$ ) in the cardiotoxicity induced untreated rats. 50mg stigmasterol treated shown significantly increased mean arterial pressure of 92 mmHg and 391 mmHg of heart rate which is equal to the control rats mean arterial pressure of 101 mmHg and 392 mmHg heart rate.

#### **Antioxidant effect of phytosterol stigmasterol on redox status in cardiotoxicity induced rats**

The TBARS and the antioxidant levels were quantified and the results were depicted in the Figure 3. Doxorubicin exposure induced lipid peroxidation which was evidenced with increased TBARS level and it was substantially decreased in the stigmasterol treated rats. Stigmasterol treatment also had a considerable impact on the glutathione system of the cardiotoxicity induced rats. It significantly ( $p < 0.05$ ) increased the concentrations of GR, GPx, GST, and GSH in the cardiotoxicity induced rats compared to the stigmasterol untreated rats. The enzymatic antioxidants SOD and CAT were significantly ( $p < 0.01$ ) diminished in the doxorubicin treated rats whereas the stigmasterol treatment significantly ( $p < 0.05$ ) elevated the SOD and CAT concentrations. 50 mg/kg of stigmasterol treated rats shown significant ( $p < 0.05$ ) increased levels of antioxidants which was comparatively equivalent to the control rats.

#### **Effect of phytosterol stigmasterol on cardiac biomarkers in cardiotoxicity induced rats**

Substantial elevation in the concentrations of aspartate aminotransferase activity and LDH activity was observed in the doxorubicin exposed treated rats compared to the other group rats. 25 mg stigmasterol were considerably decreased the AST and LDH in cardiotoxicity induced rats. 50mg stigmasterol treated and control rats shown significantly ( $p < 0.05$ ) equivalent levels of AST and LDH. Stigmasterol treatment also decreased the levels of creatinine kinase activity in

cardiotoxicity induced rats which was significantly ( $p < 0.05$ ) increased in the stigmasterol untreated rats (Fig. 4).

#### **Ameliorative effect of stigmasterol against myocardial damage induced by doxorubicin**

CK-MB, GP-BB and H-FABP were considered as biomarkers that play crucial roles in the early diagnosis and monitoring of cardiotoxicity hence the levels were detected in serum and represented in Figure 5. CK-MB, GP-BB and H-FABP levels were elevated to  $28 \pm 0.02$ ,  $61 \pm 0.03$  and  $9.8 \pm 0.03$  ng/mL in only doxorubicin treated rats compared to the control rats which exhibited  $11.87 \pm 0.008$ ,  $45.23 \pm 0.007$  and  $6.28 \pm 0.004$  respectively. Both 25 mg and 50 mg stigmasterol treated rats shown decreased levels of only doxorubicin treated rats. The levels of CK-MB, GP-BB and H-FABP were  $17.84 \pm 0.02$ ,  $53.24 \pm 0.02$  and  $8.7 \pm 0.02$  ng/mL respectively in 25mg stigmasterol treated rats and  $14.65 \pm 0.008$ ,  $48.62 \pm 0.009$  and  $7.6 \pm 0.003$  ng/mL respectively in 50 mg stigmasterol treated rats.

#### **Effect of phytosterol stigmasterol on INF- $\gamma$ and MCP-1 in cardiotoxicity induced rats**

Figure 6 illustrates the levels of cytokine Interferon  $\gamma$  and chemokine Monocyte Chemotactic Protein-1 in the cardiotoxicity induced rats. INF- $\gamma$  and MCP-1 were not detected in the control and 50mg/kg stigmasterol treated rats whereas the 25mg/kg stigmasterol treated rats exhibited  $6.7 \pm 0.04$  and  $311 \pm 1.8$  pg/mL respectively. Doxorubicin alone treated rats shown significantly ( $p < 0.05$ ) increased levels of INF- $\gamma$  ( $13.8 \pm 0.03$  pg/mL) and MCP-1 ( $414 \pm 2.5$  pg/mL) compared to the other group rats.

#### **Impact of phytosterol stigmasterol on diagnostic indicators in cardiotoxicity induced rats**

TGF- $\beta$  is a multifunctional cytokine which often elevated in response to injury or stress to the heart tissue. Doxorubicin exposure significantly ( $p < 0.01$ ) elevated the TGF- $\beta$  compared to the control rats. Stigmasterol treatment significantly diminished the TGF- $\beta$ . The sensitive diagnostic biomarkers of myocardial infraction cTroponinI, and BNP were quantified in the serum, and the results were depicted in Figure 7. Both cTroponinI, and BNP levels were substantially elevated in the doxorubicin treated rats. Stigmasterol treatment significantly ( $p < 0.05$ ) decreased the cTroponinI and BNP concentrations compared to the doxorubicin alone treated rats.

### **Effect of phytosterol stigmasterol on pro-inflammatory cytokines in cardiotoxicity induced rats**

The induction of cardiotoxicity in doxorubicin treated rats were confirmed with augmented TNF- $\alpha$ , IL-1 $\beta$ , and NF- $\kappa$ B levels compared with control. It also diminished the levels of HO-1 and NQO1 than the other group rats. Stigmasterol treatment significantly ( $p < 0.05$ ) decreased the levels of TNF- $\alpha$ , IL-1 $\beta$ , NF- $\kappa$ B and increased the HO-1 and NQO1 levels in cardiotoxicity induced rats (Fig. 8).

### **Effect of phytosterol stigmasterol on cardiac tissue histoarchitecture in cardiotoxicity induced rats**

Figure 9 depicts the representative images of hematoxylin and eosin stained cardiac tissue of experimental rats. The control group rats displayed typical cardiac tissue characteristics, characterized by a normal oval nucleus surrounded by branching striated muscle fibers positioned at the periphery (A). In contrast, the doxorubicin alone treated rats exhibited several pathological features, including numerous clogged and dilated blood arteries, excessive discharge of RBCs, edema, cytoplasmic vacuolations, reduced number of nuclei, loss of muscle fiber striation, and fragmentation accompanied by necrosis (B). However, noticeable alleviation was noted in both 25 mg/kg (C) and 50 mg/kg (D) stigmasterol treated rats.

### **Docking of Stigmasterol with NF- $\kappa$ B**

The stigmasterol was allowed to dock into the active site of NF- $\kappa$ B using the CB-Dock. It has been found that stigmasterol showed excellent binding with NF- $\kappa$ B with as Vina score of  $-6.9$ . After close inspection of docked pose in 3D, it was observed that, it was found deeply buried into the active site lined with amino acid residues ARG54, PHE55, TYR57, CYS59, GLU60, HIS141, VAL142, THR143, LYS144, ASP206, LEU207, SER208, ASP239, SER240, LYS241, ALA242, PRO243, SER246, ASN247, LYS249, ASP271, LYS272, ARG305, GLN306, and PHE307 of Chain A, and ARG54, PHE55, TYR57, CYS59, GLU60, HIS141, VAL142, THR143, LYS144, LYS145, LEU207, SER208, ASP239, LYS241, ALA242, PRO243, ASN244, LYS272, GLN274, ARG305, GLN306, and PHE307 of Chain B. As shown in Figure 10b, stigmasterol created Alkyl interaction with Lys144, Tyr57, Leu207, Ala242, Pro243 and pi-alkyl interaction with Ala242, and His141. The molecular docking analysis revealed that Stigmasterol possesses a

strong binding affinity for NF- $\kappa$ B, a key transcription factor regulating inflammation and immune responses. This robust interaction is thought to be a major contributor to its pronounced anti-inflammatory properties observed in this study. By modulating NF- $\kappa$ B activity, Stigmasterol may effectively reduce inflammatory signaling, thereby mitigating cardiotoxic effects. These findings highlight its potential as a cardioprotective agent in experimental models, aligning with previous research on its bioactive properties and therapeutic applications in inflammatory and cardiovascular conditions (Fig. 10).

## **DISCUSSION**

Doxorubicin, an anthracycline, is a pivotal chemotherapeutic drug, utilized in the treatment for a broad spectrum of solid organ tumors and hematologic malignancies, leukemia and lymphomas [15]. Despite their therapeutic efficacy, its clinical utility is hampered by significant acute and chronic toxicities specifically cardiotoxicity. While it's widely recognized that high cumulative doses of doxorubicin exceeding 400 mg/m<sup>2</sup> may induce cardiotoxicity, studies on cancer survivors, both in childhood and adulthood, have indicated that doxorubicin-induced cardiomyopathy can manifest even at cumulative doses below 400 mg/m<sup>2</sup> [28]. Acute cardiotoxicity, characterized by symptoms like arrhythmias, and chronic toxicity, which can progress to irreversible cardiomyopathy, are among the major complications associated with DOX treatment. Approximately 30–40% of patients receiving a total dose of 500 mg/m<sup>2</sup> reported to develop cardiomyopathy [21, 23].

A promising approach to mitigate cardiotoxicity in the patients undergoing chemotherapy involves the utilization of cardioprotectants or phyto-formulations. Phytochemicals, found are often well tolerated and possess potent antioxidant properties therefore they hold the potential to shield cardiac muscle from the adverse impacts of oxidative stress [14]. Phytochemicals serve as valuable repositories of pharmacophores and merit consideration as drug templates for ongoing research and development efforts aimed at addressing DOX-induced cardiotoxicity [22]. Therefore, we treated the healthy Wistar rats with 2.5 mg/kg doxorubicin in alternate days for period 2 weeks and simultaneously supplemented with stigmasterol to elucidate the efficacy of the stigmasterol to prevent cardiotoxicity induction in rats.

Cachexia is the primary symptom observed in the cancer patients undergoing chemotherapy with poor prognosis [36]. Doxorubicin deregulates both the glucose and lipid metabolism which inhibits adipogenesis and lipogenesis which eventually leads to adipose mass atrophy and body

weight [5]. Stigmasterol treatment had significantly augmented the body weight and heart relative organ weight in the doxorubicin treated which proves the efficacy of stigmasterol in inhibiting doxorubicin cardiotoxicity. Arrhythmias, one of the doxorubicin induced manifestation which may result in palpitations, sensations of dizziness, breathlessness, fainting spells, or in extreme instances, cardiac arrest was significantly reduced in the stigmasterol treatment. Stigmasterol supplemented rats shown normal heart rate, systolic and diastolic pressure which was deregulated doxorubicin alone treated rats.

Cardiomyocytes contain a significant abundance of mitochondria, which are a primary target of DOX. Compared to other tissues, cardiomyocytes exhibit an increased mitochondrial count by approximately 35–40%, potentially contributing to their susceptibility to injury. Doxorubicin reduces redox cycle causing increased ROS generation and disrupted ATP synthesis. The mitochondrial ROS synthesizing enzymes converts doxorubicin to semiquinones which reacts with oxygen to form superoxide anions or reactive oxygen species or reactive nitrogen species causes peroxidation of cell membrane lipids and aggregation of proteins. The depletion of endogenous antioxidants was also reported with doxorubicin treatment. Decreased levels of antioxidants causes oxidative damage of myocardium. Mice with GPx1 deficient are more to cardiotoxicity caused by doxorubicin than the wild type mice [16]. Stigmasterol had proven antioxidant efficacy which was reported in various carcinogenic and neurotoxicity studies. Research indicates that stigmasterol mitigates excitotoxicity, DNA injury, and mitochondrial dysfunction via inhibiting reactive oxygen species production. Moreover, stigmasterol enhances the activities of antioxidant enzymes thereby conferring neuroprotective [5]. These results correlate well with our studies that stigmasterol treatment effectively enhanced the antioxidants and prevented lipid peroxidation in doxorubicin treated rats.

Creatinine kinase, energy reservoir of the body is found in various tissue, in heart the CK-MB isoenzyme was present which reported to be increased with doxorubicin treatment. In the presence of ferrous ion, the increased CK generates peroxynitrite free radicals which damages the cardiac tissue. GP-BB and hFABP are considered to be the early diagnostic markers of myocardial injury. GPBB is the glucose provider of heart and it is found elevated during the first four hours of myocardial injury. hFABP is protein responsible for the intracellular myocardial transport it is also found to be elevated during the acute myocardial infarction [30]. Substantially elevated levels of CK, GPBB and hFABP was noted in the doxorubicin-treated rats confirming

the induction of cardiac damage whereas the rats supplemented with stigmasterol along with doxorubicin exhibited decreased CK, GPBB and hFABP levels.

Inflammatory response induced by doxorubicin was evidenced with elevated TNF- $\alpha$ , NF $\kappa$ B, IL-6, IL-8, and MCP-1 concentrations which in turn leads to cardiomyopathy and myocardial infarction [4]. Doxorubicin administration reported to elevated Interferon- $\gamma$  levels suggesting induction of inflammation [33, 35]. Stigmasterol through its anti-inflammatory action significantly decreased the INF- $\gamma$ , MCP-1 and proinflammatory cytokines TNF- $\alpha$ , NF $\kappa$ B and IL-1 $\beta$  which was remarkably increased in the doxorubicin alone treated mice. Some of Nrf2 cytoprotective targeting genes well established in oxidative stress mechanism are HO-1, NQO1 and GCLM decreased with doxorubicin treatment. HO-1 is an enzyme that catalyzes the breakdown of heme into biliverdin, carbon monoxide (CO), and iron. Biliverdin is subsequently converted into bilirubin, which possesses potent antioxidant properties [8, 10, 11]. NQO1 is an enzyme involved in the detoxification of quinones and other electrophilic compounds. It plays a critical role in protecting cells from oxidative damage by preventing the accumulation of ROS and reactive quinone metabolites [24, 26]. Stigmasterol treatment elevated the both HO-1 and NQO1 concentrations in the doxorubicin treated rats this may be the reason for increased antioxidants levels which had prevented from doxorubicin induced cardiac damage. In the cardiovascular system, TGF- $\beta$  plays a pivotal role in the process of fibrotic cardiac remodeling, which is implicated in the progression of heart failure [27, 34]. Elevated TGF- $\beta$  superfamily ligands have been increasingly associated with the advancement of heart failure [13]. The gold standard biomarker for detecting myocardial injury and cardiotoxicity is cardiac troponin, specifically cardiac troponin I (cTnI) [2, 37]. Elevated levels of cTnI in the bloodstream indicate myocardial injury and serve as a sensitive and reliable indicator with significant clinical and prognostic implications, particularly in response to chemotherapy like doxorubicin (Dox). BNP, a hormone secreted by ventricular myocytes, is another valuable marker, reflecting cardiac stress and volume overload [29]. Increased levels of BNP in plasma, observed during chemotherapy, can predict the onset of congestive heart failure, offering a predictive tool for cardiac dysfunction associated with chemotherapy-induced cardiotoxicity. Hence in this work we evaluated TGF- $\beta$ , cTnI and BNP in stigmasterol supplement doxorubicin treated rats. Stigmasterol supplementation effectively decreased the levels of TGF- $\beta$ , cTnI and BNP in doxorubicin treated rats confirming its cardioprotective effect. It was further evidenced

with our histopathological analysis. Docking studies play a crucial role in drug research by predicting molecular interactions between bioactive compounds and target proteins [25]. This computational approach helps identify potential drug candidates by assessing binding affinity, stability, and specificity. It accelerates drug discovery by reducing the need for extensive laboratory testing, guiding structure-based drug design, and optimizing lead compounds. In pharmacology, docking studies aid in understanding mechanisms of action, improving drug efficacy, and minimizing side effects [6]. By simulating ligand-protein interactions, they provide valuable insights into therapeutic potential, making them an essential tool in modern drug development and biomedical research. In this study, molecular docking analysis was performed using the CB-Dock webserver [17, 18]. Results revealed that Stigmasterol exhibits a strong binding affinity for NF- $\kappa$ B by interacting with key amino acid residues, including Lys144, Tyr57, Leu207, Ala242, Pro243, and His141 of Chain A. These interactions suggest a stable ligand-protein complex, potentially contributing to its anti-inflammatory properties. Furthermore, our findings align with previous studies, where similar ligand interactions with these residues were reported to enhance binding affinity for NF- $\kappa$ B [19, 31]. This consistency reinforces the reliability of our results and highlights Stigmasterol's potential as a promising candidate for targeting NF- $\kappa$ B-mediated inflammatory pathways.

Moreover, despite these promising results, the current study has certain limitations. For example, the present study lacks the in-depth molecular-level assays to precisely comprehend the underlying molecular mechanisms by which stigmasterol shows its cardioprotective mechanisms against doxorubicin-induced cardiotoxicity. These limitations need to be addressed in future studies.

## **CONCLUSIONS**

In this modern era, cancer has emerged as a global disease, and with advancements in the pharmaceutical field, numerous anticancer drugs have become available. One such potent anticancer drug with a long history of use is doxorubicin. However, its utility is greatly hindered by its cardiotoxicity, which limits its clinical application and compromises patient outcomes. Supplementing anticancer drugs with phytochemicals has been shown to decrease their side effects, offering a promising strategy to improve cancer treatment. In the present research, we investigated the potency of the phytochemical stigmasterol in alleviating cardiotoxicity induced

by doxorubicin. Our findings demonstrate that stigmasterol effectively inhibits the oxidative stress and inflammatory response induced by doxorubicin, thereby preventing cardiac damage in rats. The cardioprotective effect of stigmasterol was confirmed through tail-cuff plethysmography analysis, quantification of diagnostic markers, and histopathological examination. These results have significant implications for clinical practice, as they suggest that stigmasterol supplementation could be a valuable adjunct therapy to mitigate doxorubicin-induced cardiotoxicity, ultimately improving the safety and efficacy of cancer treatment. Our study provides a foundation for future clinical trials to explore the potential of stigmasterol as a cardioprotective agent, with the potential to enhance patient outcomes and improve the quality of life for cancer patients undergoing doxorubicin treatment.

## ARTICLE INFORMATION AND DECLARATIONS

### **Data availability statement**

Not applicable.

### **Ethics statement**

All work has been done under the guidelines of Institutional Ethics Committee of Inner Mongolia Autonomous Region People 's Hospital China.

### **Author contributions**

YW is the only author of this article. He is responsible for conceptualized, analysis, experiment, software, final editing and reviewing.

### **Conflict of interest**

The author declares no competing interests.

## REFERENCES

1. Abushouk AI, Ismail A, Salem AM, et al. Cardioprotective mechanisms of phytochemicals against doxorubicin-induced cardiotoxicity. *Biomed Pharmacother.* 2017; 90: 935–946, doi: [10.1016/j.biopha.2017.04.033](https://doi.org/10.1016/j.biopha.2017.04.033), indexed in Pubmed: [28460429](https://pubmed.ncbi.nlm.nih.gov/28460429/).
2. Babuin L, Jaffe AS. Troponin: the biomarker of choice for the detection of cardiac injury. *CMAJ.* 2005; 173(10): 1191–1202, doi: [10.1503/cmaj/051291](https://doi.org/10.1503/cmaj/051291), indexed in Pubmed: [16275971](https://pubmed.ncbi.nlm.nih.gov/16275971/).
3. Bakrim S, Benkhaira N, Bourais I, et al. Health benefits and pharmacological properties of stigmasterol. *Antioxidants (Basel).* 2022; 11(10), doi: [10.3390/antiox11101912](https://doi.org/10.3390/antiox11101912), indexed in Pubmed: [36290632](https://pubmed.ncbi.nlm.nih.gov/36290632/).
4. Bhagat A, Shrestha P, Kleinerman ES. The innate immune system in cardiovascular diseases and its role in doxorubicin-induced cardiotoxicity. *Int J Mol Sci.* 2022; 23(23), doi: [10.3390/ijms232314649](https://doi.org/10.3390/ijms232314649), indexed in Pubmed: [36498974](https://pubmed.ncbi.nlm.nih.gov/36498974/).
5. Biondo LA, Lima Junior EA, Souza CO, et al. Impact of doxorubicin treatment on the physiological functions of white adipose tissue. *PLoS One.* 2016; 11(3): e0151548, doi: [10.1371/journal.pone.0151548](https://doi.org/10.1371/journal.pone.0151548), indexed in Pubmed: [27015538](https://pubmed.ncbi.nlm.nih.gov/27015538/).
6. Brooijmans N, Kuntz ID. Molecular recognition and docking algorithms. *Annu Rev Biophys Biomol Struct.* 2003; 32: 335–373, doi: [10.1146/annurev.biophys.32.110601.142532](https://doi.org/10.1146/annurev.biophys.32.110601.142532), indexed in Pubmed: [12574069](https://pubmed.ncbi.nlm.nih.gov/12574069/).
7. Carneiro BA, El-Deiry WS. Targeting apoptosis in cancer therapy. *Nat Rev Clin Oncol.* 2020; 17(7): 395–417, doi: [10.1038/s41571-020-0341-y](https://doi.org/10.1038/s41571-020-0341-y), indexed in Pubmed: [32203277](https://pubmed.ncbi.nlm.nih.gov/32203277/).
8. Chau LY. Heme oxygenase-1: emerging target of cancer therapy. *J Biomed Sci.* 2015; 22(1): 22, doi: [10.1186/s12929-015-0128-0](https://doi.org/10.1186/s12929-015-0128-0), indexed in Pubmed: [25885228](https://pubmed.ncbi.nlm.nih.gov/25885228/).
9. Chen WP, Yu C, Hu PF, et al. Stigmasterol blocks cartilage degradation in rabbit model of osteoarthritis. *Acta Biochim Pol.* 2012; 59(4): 537–541, indexed in Pubmed: [23074702](https://pubmed.ncbi.nlm.nih.gov/23074702/).
10. Chiang SK, Chen SE, Chang LC. A dual role of heme oxygenase-1 in cancer cells. *Int J Mol Sci.* 2018; 20(1), doi: [10.3390/ijms20010039](https://doi.org/10.3390/ijms20010039), indexed in Pubmed: [30583467](https://pubmed.ncbi.nlm.nih.gov/30583467/).

11. Chiang SK, Chen SE, Chang LC. The role of HO-1 and its crosstalk with oxidative stress in cancer cell survival. *Cells*. 2021; 10(9), doi: [10.3390/cells10092401](https://doi.org/10.3390/cells10092401), indexed in Pubmed: [34572050](https://pubmed.ncbi.nlm.nih.gov/34572050/).
12. Ferlay J, Colombet M, Soerjomataram I, et al. Estimating the global cancer incidence and mortality in 2018: GLOBOCAN sources and methods. *Int J Cancer*. 2019; 144(8): 1941–1953, doi: [10.1002/ijc.31937](https://doi.org/10.1002/ijc.31937), indexed in Pubmed: [30350310](https://pubmed.ncbi.nlm.nih.gov/30350310/).
13. Hanna A, Frangogiannis NG. The role of the TGF- $\beta$  superfamily in myocardial infarction. *Front Cardiovasc Med*. 2019; 6: 140, doi: [10.3389/fcvm.2019.00140](https://doi.org/10.3389/fcvm.2019.00140), indexed in Pubmed: [31620450](https://pubmed.ncbi.nlm.nih.gov/31620450/).
14. Kant UR. Antihyperlipidemic and cardioprotective effects of plant natural products: a review. *Int J Green Pharm*. 2021; 15(1): 1–19.
15. Kciuk M, Gielecińska A, Mujwar S, et al. Doxorubicin — an agent with multiple mechanisms of anticancer activity. *Cells*. 2023; 12(4), doi: [10.3390/cells12040659](https://doi.org/10.3390/cells12040659), indexed in Pubmed: [36831326](https://pubmed.ncbi.nlm.nih.gov/36831326/).
16. Liu C, Ma X, Zhuang J, et al. Cardiotoxicity of doxorubicin-based cancer treatment: What is the protective cognition that phytochemicals provide us? *Pharmacol Res*. 2020; 160: 105062, doi: [10.1016/j.phrs.2020.105062](https://doi.org/10.1016/j.phrs.2020.105062), indexed in Pubmed: [32652197](https://pubmed.ncbi.nlm.nih.gov/32652197/).
17. Liu Y, Grimm M, Dai WT, et al. CB-Dock: a web server for cavity detection-guided protein-ligand blind docking. *Acta Pharmacol Sin*. 2020; 41(1): 138–144, doi: [10.1038/s41401-019-0228-6](https://doi.org/10.1038/s41401-019-0228-6), indexed in Pubmed: [31263275](https://pubmed.ncbi.nlm.nih.gov/31263275/).
18. Liu Y, Yang X, Gan J, et al. CB-Dock2: improved protein-ligand blind docking by integrating cavity detection, docking and homologous template fitting. *Nucleic Acids Res*. 2022; 50(W1): W159–W164, doi: [10.1093/nar/gkac394](https://doi.org/10.1093/nar/gkac394), indexed in Pubmed: [35609983](https://pubmed.ncbi.nlm.nih.gov/35609983/).
19. Masih A, Agnihotri AK, Srivastava JK, et al. Discovery of novel pyrazole derivatives as a potent anti-inflammatory agent in RAW264.7 cells via inhibition of NF- $\kappa$ B for possible benefit against SARS-CoV-2. *J Biochem Mol Toxicol*. 2021; 35(3): e22656, doi: [10.1002/jbt.22656](https://doi.org/10.1002/jbt.22656), indexed in Pubmed: [33094891](https://pubmed.ncbi.nlm.nih.gov/33094891/).

20. Mohammadi M, Arabi L, Alibolandi M. Doxorubicin-loaded composite nanogels for cancer treatment. *J Control Release*. 2020; 328: 171–191, doi: [10.1016/j.jconrel.2020.08.033](https://doi.org/10.1016/j.jconrel.2020.08.033), indexed in Pubmed: [32866591](https://pubmed.ncbi.nlm.nih.gov/32866591/).
21. Nabati M, Janbabai G, Baghyari S, et al. Cardioprotective effects of carvedilol in inhibiting doxorubicin-induced cardiotoxicity. *J Cardiovasc Pharmacol*. 2017; 69(5): 279–285, doi: [10.1097/FJC.0000000000000470](https://doi.org/10.1097/FJC.0000000000000470), indexed in Pubmed: [28141699](https://pubmed.ncbi.nlm.nih.gov/28141699/).
22. Othman S, Lum P, Gan S, et al. Protective effect of natural products against chemotherapy-induced cardiotoxicity: a review. *Pharmacog J*. 2020; 12(5): 1180–1189, doi: [10.5530/pj.2020.12.166](https://doi.org/10.5530/pj.2020.12.166).
23. Octavia Y, Tocchetti CG, Gabrielson KL, et al. Doxorubicin-induced cardiomyopathy: from molecular mechanisms to therapeutic strategies. *J Mol Cell Cardiol*. 2012; 52(6): 1213–1225, doi: [10.1016/j.yjmcc.2012.03.006](https://doi.org/10.1016/j.yjmcc.2012.03.006), indexed in Pubmed: [22465037](https://pubmed.ncbi.nlm.nih.gov/22465037/).
24. Oh ET, Park HJ. Implications of NQO1 in cancer therapy. *BMB Rep*. 2015; 48(11): 609–617, doi: [10.5483/bmbrep.2015.48.11.190](https://doi.org/10.5483/bmbrep.2015.48.11.190), indexed in Pubmed: [26424559](https://pubmed.ncbi.nlm.nih.gov/26424559/).
25. Pagadala NS, Syed K, Tuszynski J. Software for molecular docking: a review. *Biophys Rev*. 2017; 9(2): 91–102, doi: [10.1007/s12551-016-0247-1](https://doi.org/10.1007/s12551-016-0247-1), indexed in Pubmed: [28510083](https://pubmed.ncbi.nlm.nih.gov/28510083/).
26. Preethi S, Arthiga K, Patil AB, et al. Review on NAD(P)H dehydrogenase quinone 1 (NQO1) pathway. *Mol Biol Rep*. 2022; 49(9): 8907–8924, doi: [10.1007/s11033-022-07369-2](https://doi.org/10.1007/s11033-022-07369-2), indexed in Pubmed: [35347544](https://pubmed.ncbi.nlm.nih.gov/35347544/).
27. Ruiz-Ortega M, Rodríguez-Vita J, Sanchez-Lopez E, et al. TGF-beta signaling in vascular fibrosis. *Cardiovasc Res*. 2007; 74(2): 196–206, doi: [10.1016/j.cardiores.2007.02.008](https://doi.org/10.1016/j.cardiores.2007.02.008), indexed in Pubmed: [17376414](https://pubmed.ncbi.nlm.nih.gov/17376414/).
28. Sheibani M, Azizi Y, Shayan M, et al. Doxorubicin-induced cardiotoxicity: an overview on pre-clinical therapeutic approaches. *Cardiovasc Toxicol*. 2022; 22(4): 292–310, doi: [10.1007/s12012-022-09721-1](https://doi.org/10.1007/s12012-022-09721-1), indexed in Pubmed: [35061218](https://pubmed.ncbi.nlm.nih.gov/35061218/).

29. Skovgaard D, Hasbak P, Kjaer A. BNP predicts chemotherapy-related cardiotoxicity and death: comparison with gated equilibrium radionuclide ventriculography. *PLoS One*. 2014; 9(5): e96736, doi: [10.1371/journal.pone.0096736](https://doi.org/10.1371/journal.pone.0096736), indexed in Pubmed: [24800827](https://pubmed.ncbi.nlm.nih.gov/24800827/).
30. Songbo M, Lang H, Xinyong C, et al. Oxidative stress injury in doxorubicin-induced cardiotoxicity. *Toxicol Lett*. 2019; 307: 41–48, doi: [10.1016/j.toxlet.2019.02.013](https://doi.org/10.1016/j.toxlet.2019.02.013), indexed in Pubmed: [30817977](https://pubmed.ncbi.nlm.nih.gov/30817977/).
31. Srivastava J, Awatade N, Bhat H, et al. Pharmacological evaluation of hybrid thiazolidin-4-one-1,3,5-triazines for NF- $\kappa$ B, biofilm and CFTR activity. *RSC Advances*. 2015; 5(108): 88710–88718, doi: [10.1039/c5ra09250g](https://doi.org/10.1039/c5ra09250g).
32. Sung H, Ferlay J, Siegel RL, et al. Global Cancer Statistics 2020: GLOBOCAN estimates of incidence and mortality worldwide for 36 cancers in 185 countries. *CA Cancer J Clin*. 2021; 71(3): 209–249, doi: [10.3322/caac.21660](https://doi.org/10.3322/caac.21660), indexed in Pubmed: [33538338](https://pubmed.ncbi.nlm.nih.gov/33538338/).
33. Syukri A, Hatta M, Amir M, et al. Doxorubicin induced immune abnormalities and inflammatory responses via HMGB1, HIF1- $\alpha$  and VEGF pathway in progressive of cardiovascular damage. *Ann Med Surg (Lond)*. 2022; 76: 103501, doi: [10.1016/j.amsu.2022.103501](https://doi.org/10.1016/j.amsu.2022.103501), indexed in Pubmed: [35340325](https://pubmed.ncbi.nlm.nih.gov/35340325/).
34. Tie Y, Tang F, Peng D, et al. TGF-beta signal transduction: biology, function and therapy for diseases. *Mol Biomed*. 2022; 3(1): 45, doi: [10.1186/s43556-022-00109-9](https://doi.org/10.1186/s43556-022-00109-9), indexed in Pubmed: [36534225](https://pubmed.ncbi.nlm.nih.gov/36534225/).
35. Wang L, Chen Q, Qi H, et al. Doxorubicin-Induced systemic inflammation is driven by upregulation of toll-like receptor TLR4 and endotoxin leakage. *Cancer Res*. 2016; 76(22): 6631–6642, doi: [10.1158/0008-5472.CAN-15-3034](https://doi.org/10.1158/0008-5472.CAN-15-3034), indexed in Pubmed: [27680684](https://pubmed.ncbi.nlm.nih.gov/27680684/).
36. Webster JM, Kempen LJ, Hardy RS, et al. Inflammation and skeletal muscle wasting during cachexia. *Front Physiol*. 2020; 11: 597675, doi: [10.3389/fphys.2020.597675](https://doi.org/10.3389/fphys.2020.597675), indexed in Pubmed: [33329046](https://pubmed.ncbi.nlm.nih.gov/33329046/).
37. Wells SM, Sleeper M. Cardiac troponins. *J Vet Emerg Critical Care*. 2008; 18(3): 235–245, doi: [10.1111/j.1476-4431.2008.00307.x](https://doi.org/10.1111/j.1476-4431.2008.00307.x).

38. Zhang J, Yang PL, Gray NS. Targeting cancer with small molecule kinase inhibitors. *Nat Rev Cancer*. 2009; 9(1): 28–39, doi: [10.1038/nrc2559](https://doi.org/10.1038/nrc2559), indexed in Pubmed: [19104514](https://pubmed.ncbi.nlm.nih.gov/19104514/).
39. Zhang X, Wang J, Zhu L, et al. Advances in stigmasterol on its anti-tumor effect and mechanism of action. *Front Oncol*. 2022; 12: 1101289, doi: [10.3389/fonc.2022.1101289](https://doi.org/10.3389/fonc.2022.1101289), indexed in Pubmed: [36578938](https://pubmed.ncbi.nlm.nih.gov/36578938/).
40. Zhang YW, Shi J, Li YJ, et al. Cardiomyocyte death in doxorubicin-induced cardiotoxicity. *Arch Immunol Ther Exp*. 2009; 57(6): 435–445, doi: [10.1007/s00005-009-0051-8](https://doi.org/10.1007/s00005-009-0051-8), indexed in Pubmed: [19866340](https://pubmed.ncbi.nlm.nih.gov/19866340/).

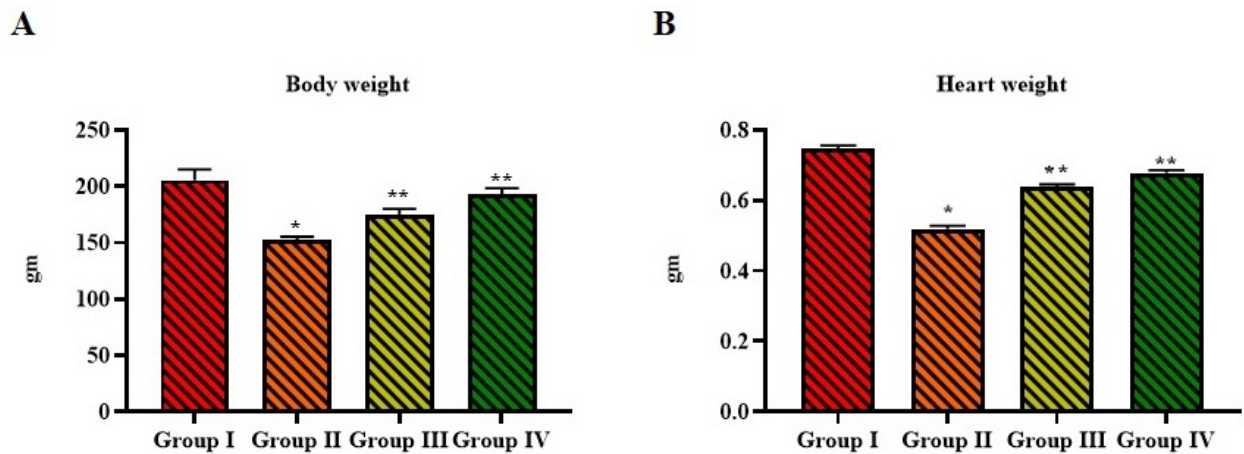


**Figure 1.** Impact of phytosterol stigmasterol on weight gain in cardiotoxicity induced mice. **A.** Total body weight. **B.** Heart weight. Data analysis utilized GraphPad Prism software (version 8.1), expressing results as mean  $\pm$  SD. Statistical significance was assessed via one-way ANOVA followed by Tukey's test, considering  $p \leq 0.05$  significant. \*Control vs doxorubicin alone treated group. \*\*Doxorubicin alone treated group vs 25 mg/kg and 50 mg/kg stigmasterol treated rats.

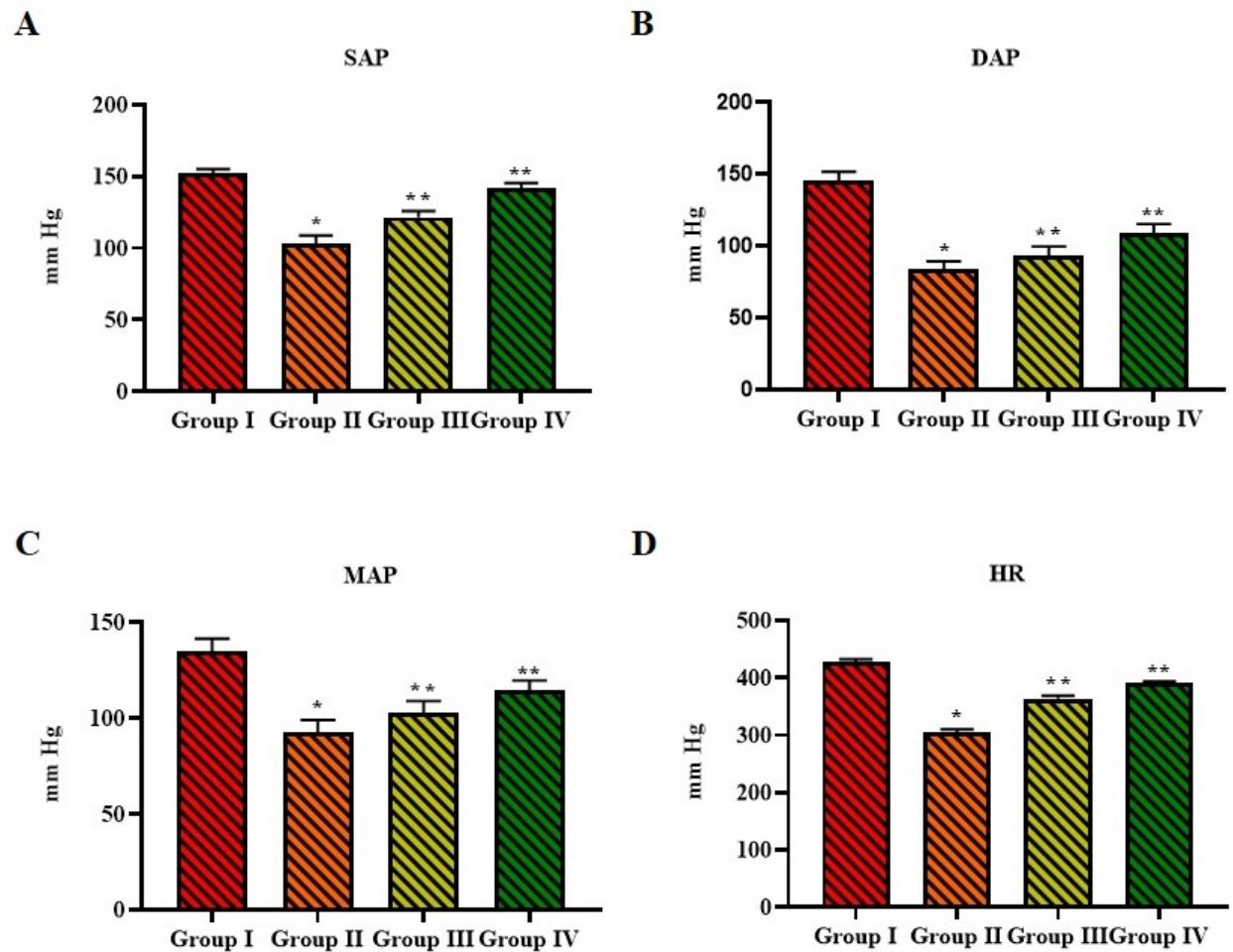


**Figure 2.** Effect of phytosterol stigmasterol on cardiac functioning in cardiotoxicity induced mice. **A.** Systolic arterial pressure (SAP); **B.** Diastolic arterial pressure (DAP); **C.** Mean arterial pressure (MAP), **D.** Heart rate (HR) detected with tail-cuff plethysmography. Data analysis utilized GraphPad Prism software (version 8.1), expressing results as mean  $\pm$  standard deviation. Statistical significance was assessed via one-way ANOVA followed by Tukey's test, considering  $p \leq 0.05$  significant. \*Control vs doxorubicin alone treated group. \*\*Doxorubicin alone treated group vs 25 mg/kg and 50 mg/kg stigmasterol treated rats.

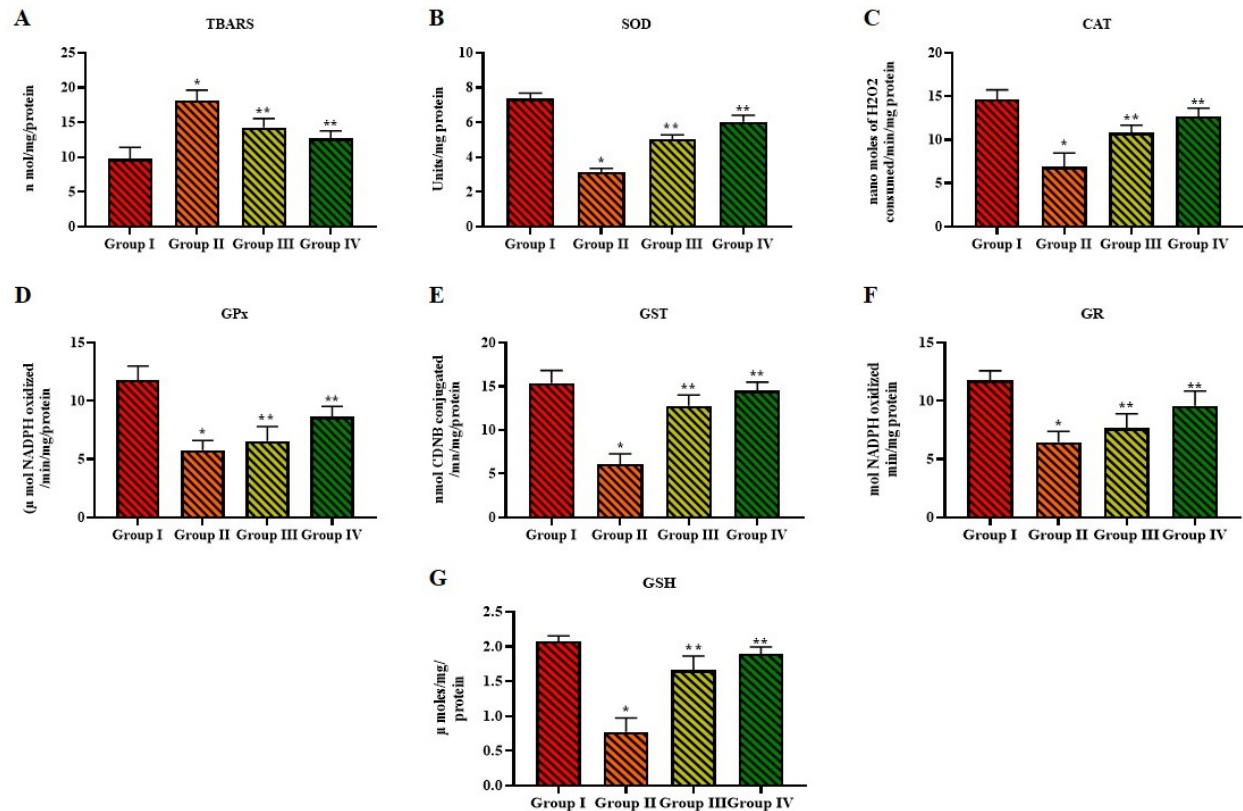


**Figure 3.** Antioxidant effect phytosterol stigmasterol on redox status in cardiotoxicity induced rats. **A.** Thiobarbituric acid reactive substance (TBARS); **B.** Superoxide dismutase (SOD); **C.** Catalase (CAT); **D.** Glutathione peroxidase (GPx); **E.** Glutathione S transferase (GST); **F.** Glutathione reductase (GR); **G.** Reduced glutathione (GSH) using colorimetric assay kits. Data analysis utilized GraphPad Prism software (version 8.1), expressing results as mean  $\pm$  standard deviation. Statistical significance was assessed via one-way ANOVA followed by Tukey's test, considering  $p \leq 0.05$  significant. \*Control vs doxorubicin alone treated group. \*\*Doxorubicin alone treated group vs 25 mg/kg and 50 mg/kg stigmasterol treated rats.

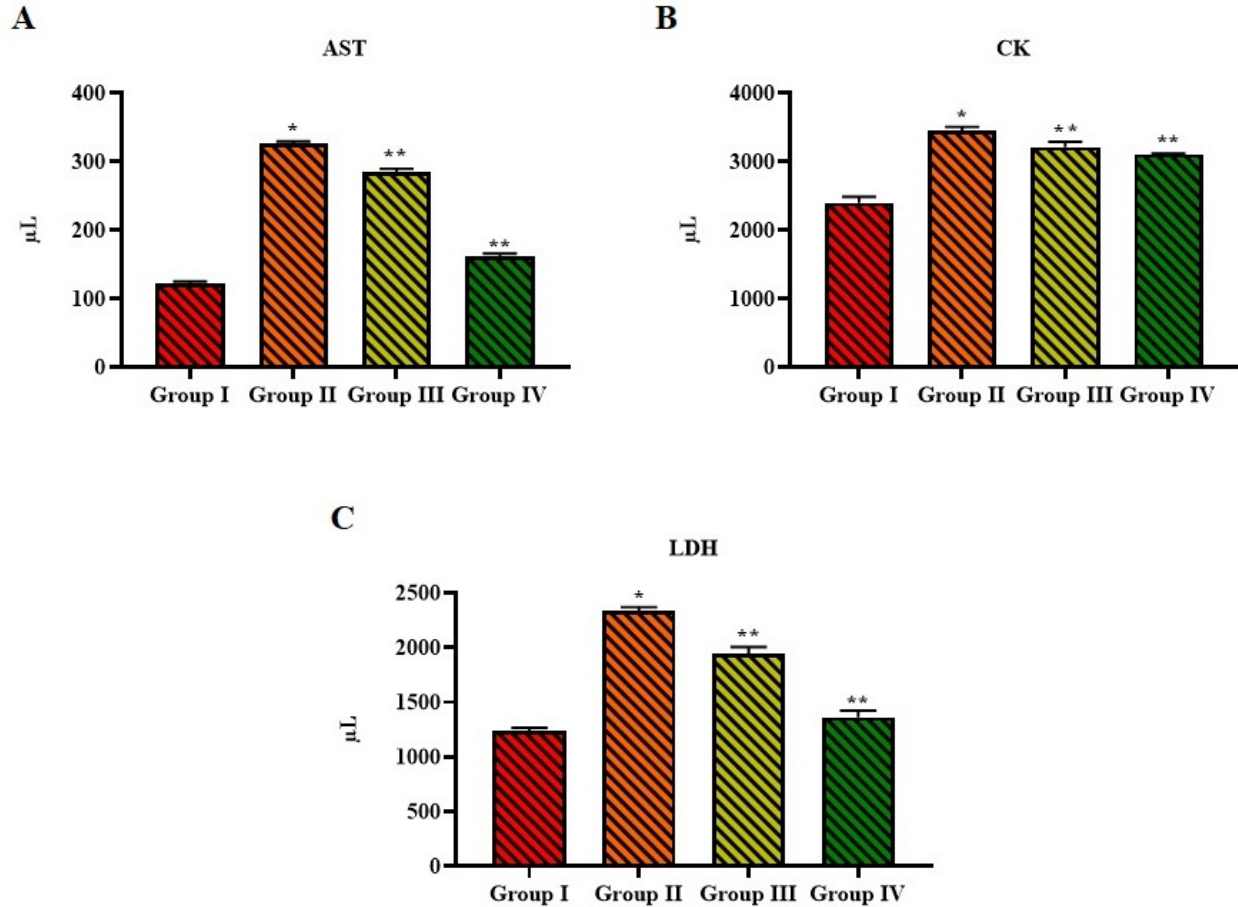


**Figure 4.** Effect of phytosterol stigmasterol on cardiac biomarkers in cardiotoxicity induced rats. **A.** Aspartate aminotransferase activity (AST); **B.** Creatinine kinase (CK); **C.** Lactate dehydrogenase (LDH) using colorimetric assay kits. Data analysis utilized GraphPad Prism software (version 8.1), expressing results as mean  $\pm$  standard deviation. Statistical significance was assessed via one-way ANOVA followed by Tukey's test, considering  $p \leq 0.05$  significant. \*Control vs doxorubicin alone treated group. \*\*Doxorubicin alone treated group vs 25 mg/kg and 50 mg/kg stigmasterol treated rats.

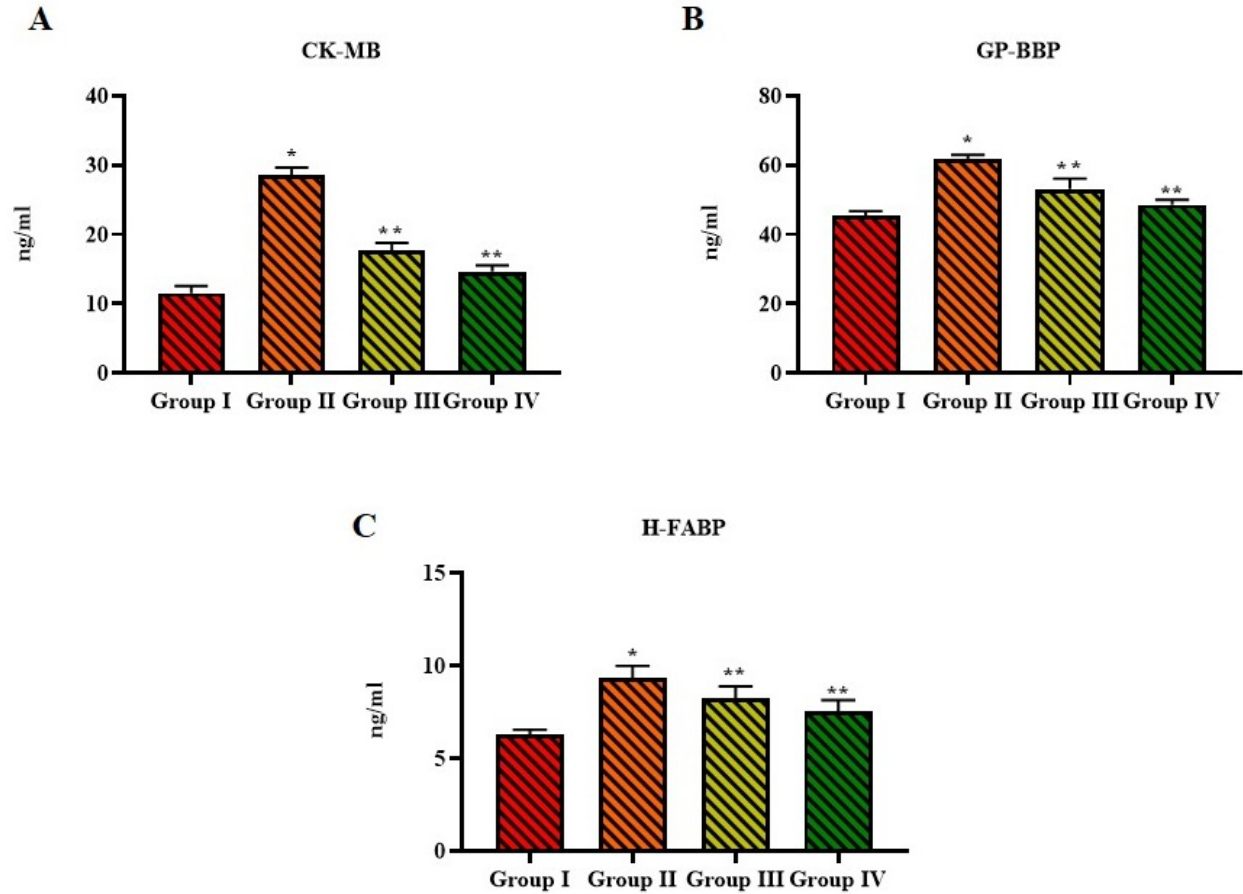


**Figure 5.** Ameliorative effect of stigmasterol phytosterol against myocardial damage induced by doxorubicin. **A.** Creatine kinase MB enzyme (CK-MB); **B.** Glycogen phosphorylase isoenzyme BB (GP-BB); **C.** Heart-type fatty acid-binding protein (H-FABP) using ELISA technique. Data analysis utilized GraphPad Prism software (version 8.1), expressing results as mean  $\pm$  standard deviation. Statistical significance was assessed via one-way ANOVA followed by Tukey's test, considering  $p \leq 0.05$  significant. \*Control vs doxorubicin alone treated group. \*\*Doxorubicin alone treated group vs 25 mg/kg and 50 mg/kg stigmasterol treated rats.

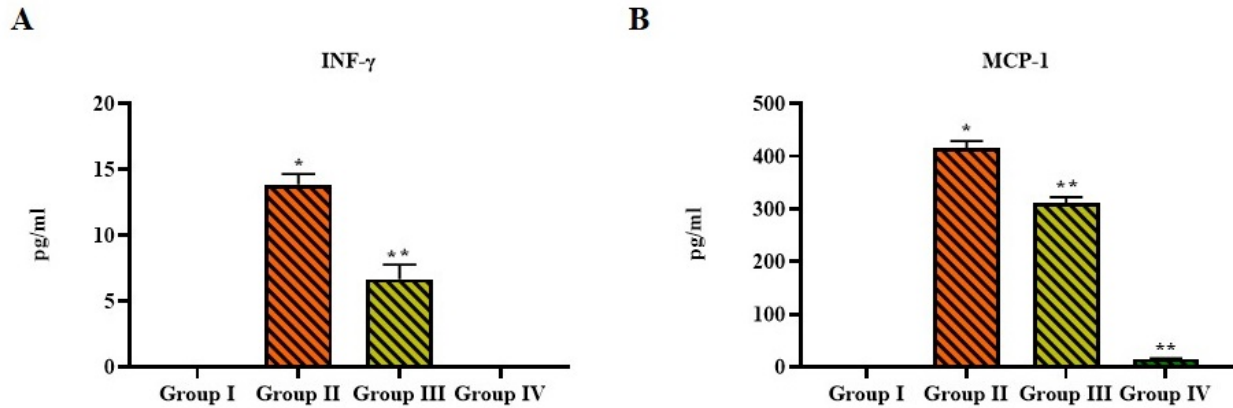


**Figure 6.** Effect of phytosterol stigmasterol on INF- $\gamma$  and MCP-1 in cardiotoxicity induced rats. **A.** Interferon  $\gamma$  (INF- $\gamma$ ); **B.** Monocyte chemotactic protein-1 (MCP-1) using ELISA technique. Data analysis utilized GraphPad Prism software (version 8.1), expressing results as mean  $\pm$  standard deviation. Statistical significance was assessed via one-way ANOVA followed by Tukey's test, considering  $p \leq 0.05$  significant. \*Control vs doxorubicin alone treated group. \*\*Doxorubicin alone treated group vs 25 mg/kg and 50 mg/kg stigmasterol treated rats.

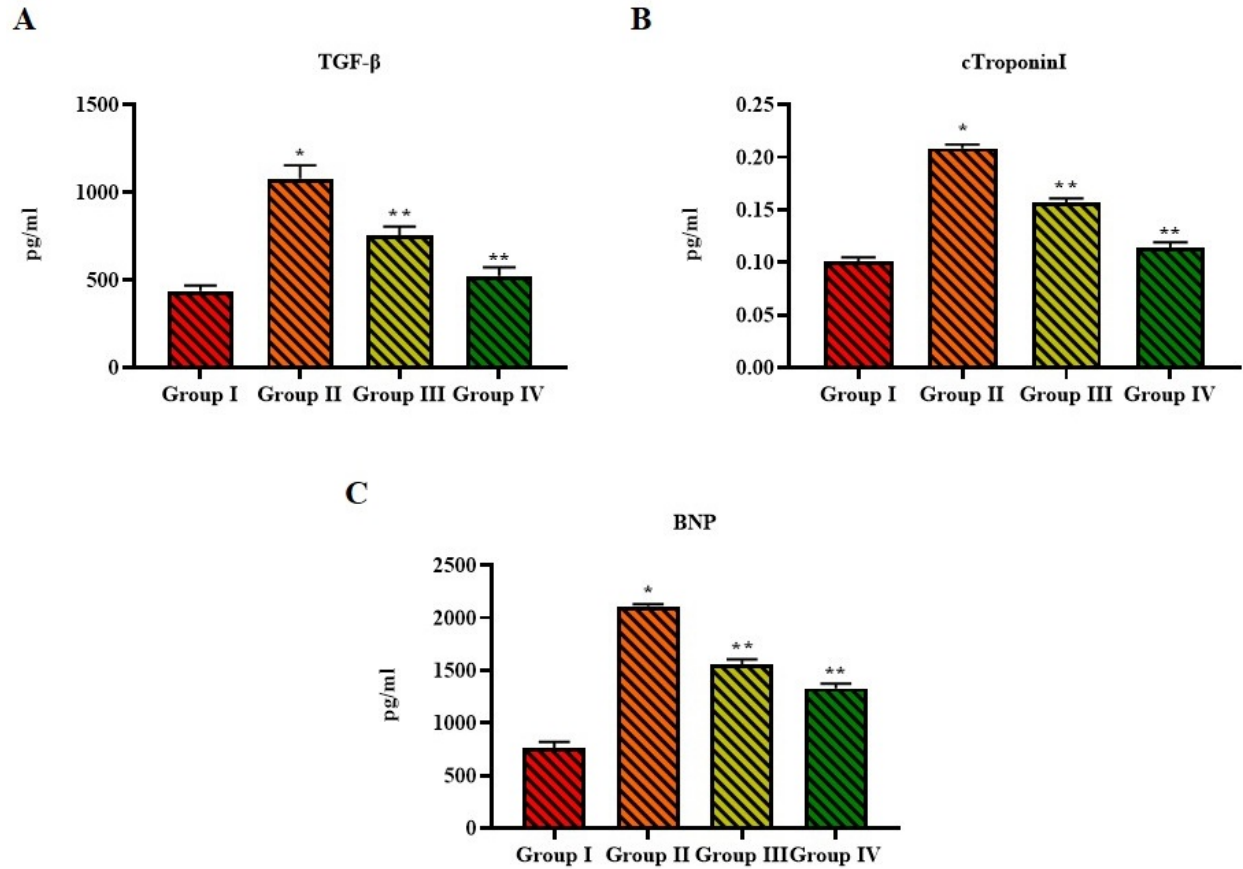


**Figure 7.** Impact of phytosterol stigmasterol on diagnostic indicators in cardiotoxicity induced rats. **A.** TGF- $\beta$ ; **B.** Cardiac troponin-I (cTnI); **C.** Brain natriuretic peptide (BNP) using ELISA technique. Data analysis utilized GraphPad Prism software (version 8.1), expressing results as mean  $\pm$  standard deviation. Statistical significance was assessed via one-way ANOVA followed by Tukey's test, considering  $p \leq 0.05$  significant. \*Control vs doxorubicin alone treated group. \*\*Doxorubicin alone treated group vs 25 mg/kg and 50 mg/kg stigmasterol treated rats.

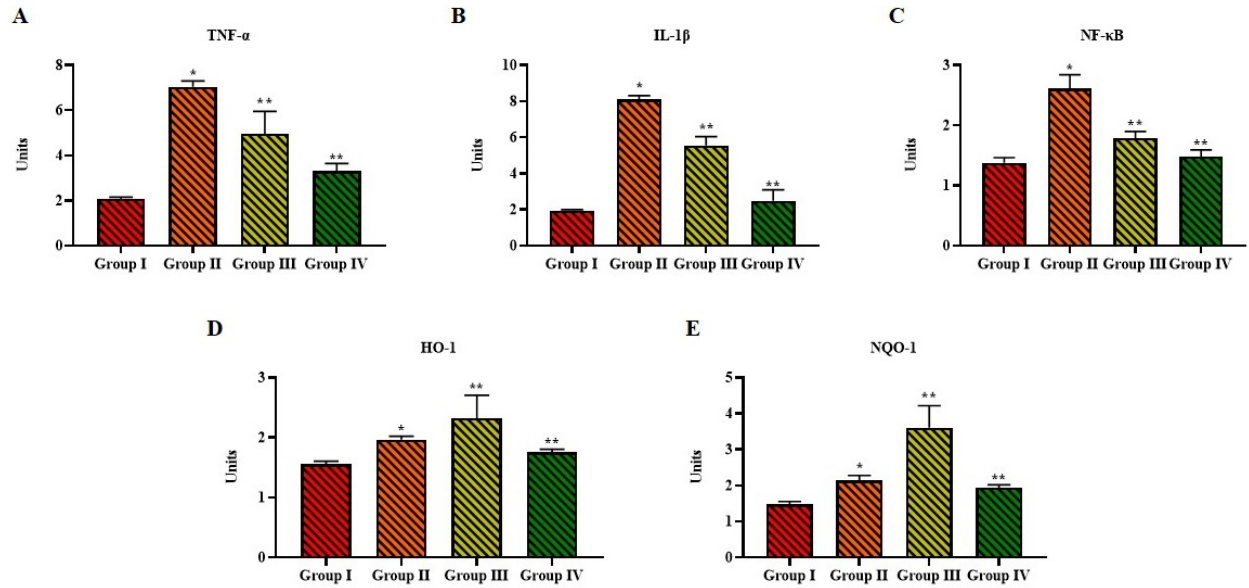


**Figure 8.** Effect of phytosterol stigmasterol on pro-inflammatory cytokines in cardiotoxicity induced rats. **A.** Tumor necrosis factor  $\alpha$  (TNF- $\alpha$ ); **B.** Interleukin 1 $\beta$  (IL-1 $\beta$ ); **C.** Nuclear factor kappa B (NF- $\kappa$ B ); **D.** Heme oxygenase (HO-1); **E.** Quinone oxidoreductase 1 (NQO1) using ELISA technique. Data analysis utilized GraphPad Prism software (version 8.1), expressing results as mean  $\pm$  standard deviation. Statistical significance was assessed via one-way ANOVA followed by Tukey's test, considering  $p \leq 0.05$  significant. \*Control vs doxorubicin alone treated group. \*\*Doxorubicin alone treated group vs 25 mg/kg and 50 mg/kg stigmasterol treated rats.

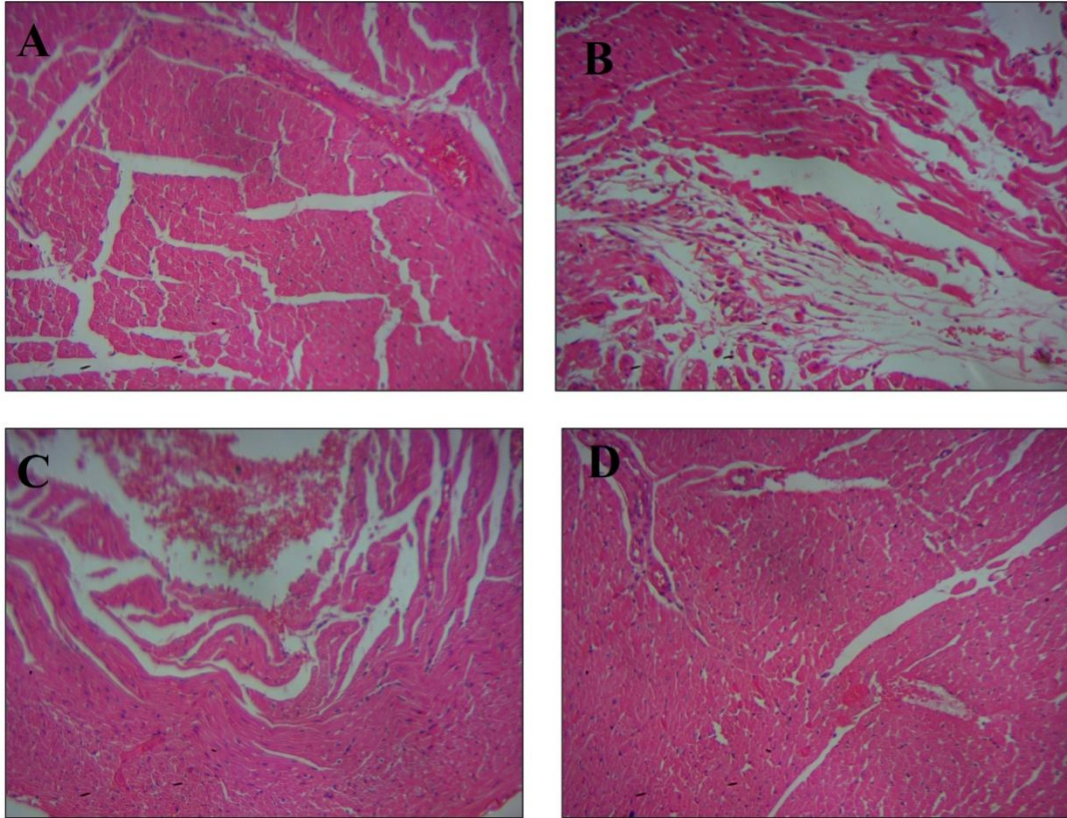


**Figure 9.** Effect of phytosterol stigmasterol on cardiac tissue histoarchitecture in cardiotoxicity induced rats. **A.** Control; **B.** 2.5 mg/kg doxorubicin alone treated group; **C.** 2.5 mg/kg doxorubicin + 25 mg/kg stigmasterol treated; **D.** 2.5 mg/kg doxorubicin + 50 mg/kg stigmasterol treated.

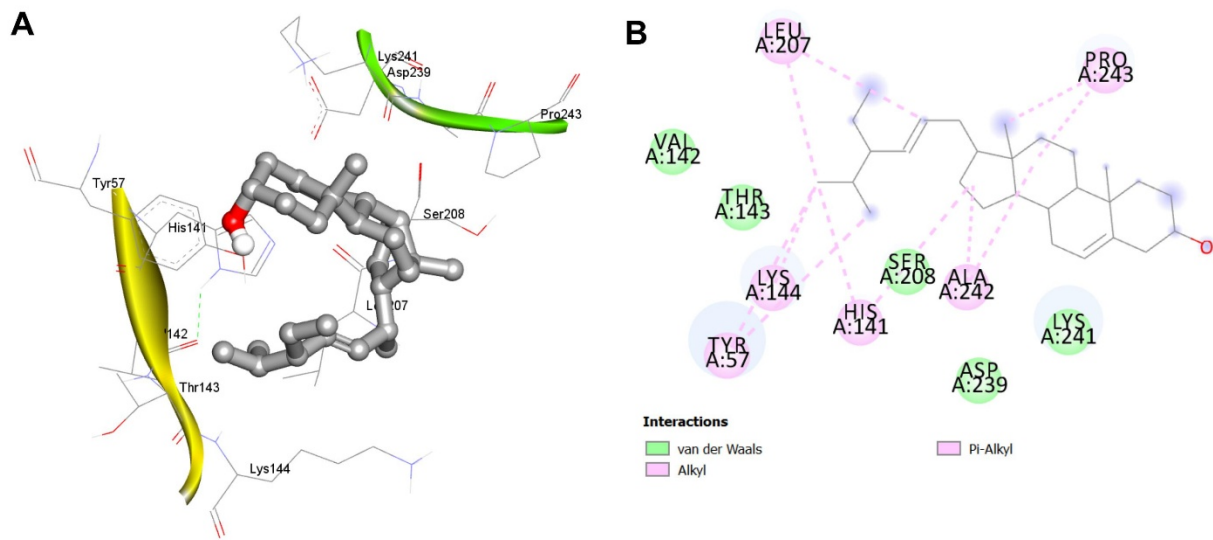


**Figure 10A.** 3D docked orientation; **B.** 2D docked orientation of stigmasterol in NF- $\kappa$ B.